# Mice with a targeted mutation in the thyroid hormone $\beta$ receptor gene exhibit impaired growth and resistance to thyroid hormone

**Masahiro Kaneshige*, Kumiko Kaneshige*, Xu-guang Zhu*, Alexandra Dace*, Lisa Garrett†, Todd A. Carter‡, Rasa Kazlauskaite§, Daniel G. Pankratz‡, Anthony Wynshaw-Boris†, Samuel Refetoff¶, Bruce Weintraub§, Mark C. Willingham‖, Carrolee Barlow‡, and Sheue-yann Cheng*,****

*Laboratory of Molecular Biology, National Cancer Institute, and †Genetic Disease Research Branch, National Human Genome Research Institute, National Institutes of Health, Bethesda, MD 20892; ‡Laboratory of Genetics, The Salk Institute for Biological Studies, La Jolla, CA 92037; §Laboratory of Molecular Endocrinology, Institute of Human Virology, Baltimore, MD 21201; ¶Department of Medicine and Pediatrics, The University of Chicago, Chicago, IL 60637; and ‖Department of Pathology, Wake Forest University School of Medicine, Winston-Salem, NC 27157

Edited by Donald D. Brown, Carnegie Institution of Washington, Baltimore, MD, and approved September 8, 2000 (received for review June 21, 2000)

**Patients with mutations in the thyroid hormone receptor $\beta$ (*TR$\beta$*) gene manifest resistance to thyroid hormone (RTH), resulting in a constellation of variable phenotypic abnormalities. To understand the molecular basis underlying the action of mutant TR$\beta$ *in vivo*, we generated mice with a targeted mutation in the *TR$\beta$* gene (*TR$\beta$PV*; PV, mutant thyroid hormone receptor kindred PV) by using homologous recombination and the *Cre*/*lox*P system. Mice expressing a single *PV* allele showed the typical abnormalities of thyroid function found in heterozygous humans with RTH. Homozygous *PV* mice exhibit severe dysfunction of the pituitary–thyroid axis, impaired weight gains, and abnormal bone development. This phenotype is distinct from that seen in mice with a null mutation in the *TR$\beta$* gene. Importantly, we identified abnormal expression patterns of several genes in tissues of *TR$\beta$PV* mice, demonstrating the interference of the mutant TR with the gene regulatory functions of the wild-type TR *in vivo*. These results show that the actions of mutant and wild-type TR$\beta$ *in vivo* are distinct. This model allows further study of the molecular action of mutant TR *in vivo*, which could lead to better treatment for RTH patients.**

The thyroid hormone 3,3′,5-triiodo-L-thyronine (T3) regulates growth, development, and differentiation. Its actions are mainly mediated through thyroid hormone receptors (TRs), which are ligand-dependent transcription factors (1, 2). Three ligand-activated TR isoforms have been identified, TR$\alpha$1, TR$\beta$1, and TR$\beta$2, which are derived from the *TR$\alpha$* and *TR$\beta$* genes, respectively. Each TR isoform has a unique developmental and tissue-specific expression (1, 2). TR binds to specific DNA sequences known as thyroid hormone response elements (TRE) in the promoter regions of T3 target genes. The transcriptional activity of TR depends not only on the types of TRE but also on a host of coregulatory proteins (3).

RTH is a syndrome characterized by reduced sensitivity of tissues to the action of thyroid hormone. This condition is characterized by elevated levels of circulating thyroid hormones associated with normal or high levels of serum thyroid-stimulating hormone (TSH) (4). The most common form of RTH is familial with autosomal dominant inheritance (4). Patients are usually heterozygotes with only one mutant *TR$\beta$* gene, and the symptoms are mild. Moreover, clinical manifestations are variable among families with RTH and also among affected family members. Some of the clinical features that have been reported include goiter, short stature, decreased weight, tachycardia, hearing loss, attention deficit–hyperactivity disorder, decreased IQ, and dyslexia (4). One single patient homozygous for a mutant *TR$\beta$* has been reported (5). This patient displayed a complex phenotype of extreme RTH with very high levels of thyroid hormone and TSH. Most TR$\beta$ mutants derived from RTH patients have reduced T3-binding affinities and transcriptional capacities. These TR$\beta$ mutants exhibit a dominant-negative effect when cotransfected with wild-type TRs (6, 7). TR$\beta$ mutants that have defects in the interaction with corepressors and coactivators have also been reported (8, 9).

Several transgenic mouse models expressing *TR$\beta$1* mutants have been developed, with the aim of understanding the mechanisms of action of TR$\beta$1 mutants *in vivo* (10–14). However, these mouse models were generated by using heterologous promoters resulting in mild phenotypes (10, 11, 14) and the expression of the mutants restricted to specific organs (11–14). The restrictive expression prevents comprehensive understanding of the action of TR$\beta$1 mutants in a physiological context. We therefore generated mice with a targeted *TR$\beta$* mutation (mutant *PV*) by using homologous recombination and the *Cre*/*lox*P system. *PV* was derived from a patient with severe RTH characterized by elevated thyroid hormone levels accompanied by normal TSH, short stature, goiter, and tachycardia (15). *PV* has an unusual mutation in exon 10, a C-insertion at codon 448, which produces a frameshift of the carboxyl-terminal 14 amino acids of TR$\beta$1 (15). This naturally occurring mutation was chosen for two reasons. First, *in vitro* characterization of PV mutant showed completely lost T3-binding and transactivation activities. PV also strongly interferes with the transactivation activity of wild-type TRs *in vitro*. Therefore, this *TR$\beta$* mutant is more likely to produce phenotypic changes in the mouse. Second, unlike the missense mutations or single amino acid deletion of *TR$\beta$* found in other patients, this unique frame-shifted mutated sequence is immunogenic, for which high-affinity specific antibodies have been developed (16). These antibodies should allow us to ask questions such as whether there is a correlation of the severity of RTH with the level of expression of mutant protein in affected tissues.

The present study shows that consistent with the findings in RTH patients, the pituitary–thyroid axis was mildly impaired in heterozygous $TR\beta^{PV/+}$ mice and severely affected in homozygous $TR\beta^{PV/PV}$ mice. $TR\beta^{PV/PV}$ mice also manifest impaired weight gain and delayed bone development. Several genes in the affected tissues of *TR$\beta$PV* mice were shown to have abnormal

This paper was submitted directly (Track II) to the PNAS office.

Abbreviation: T3, 3,3′,5-triiodo-L-thyronine; T4, L-thyroxine; TR, thyroid hormone receptor; TRE, thyroid hormone response element; TR$\beta$1, TR subtype $\beta$1; RTH, resistance to thyroid hormone; PV, mutant thyroid hormone receptor kindred PV; TSH, thyroid-stimulating hormone; 5′-DI-I, 5′-deiodinase-I; RT, reverse transcription; GH, growth hormone; ME, malic enzyme; $\alpha$-SU, $\alpha$-glycoprotein subunit.

**To whom reprint requests should be addressed at: Building 37, Room 2D24, 37 Convent Drive, MSC 4255, Bethesda, MD 20892-4255. E-mail: sycheng@helix.nih.gov.

The publication costs of this article were defrayed in part by page charge payment. This article must therefore be hereby marked "*advertisement*" in accordance with 18 U.S.C. §1734 solely to indicate this fact.

Article published online before print: *Proc. Natl. Acad. Sci. USA*, 10.1073/pnas.230285997. Article and publication date are at www.pnas.org/cgi/doi/10.1073/pnas.230285997

expression patterns, demonstrating the *in vivo* interference of the mutant TR$\beta$ with the gene regulatory functions of the wild-type receptors.

## Materials and Methods

**Preparation of PV Mutant Mice.** A *TR$\beta$* mouse genomic clone was isolated from an ES-129 P1 Library (Genome Systems, St. Louis) by using primers specific for the *TR$\beta$* gene. After mapping the genomic sequences in the regions of exons 8, 9, 10 and the down-stream sequences of exon 10, a 17.5-kb targeting vector was constructed (see Fig. 1*A*). A PV mutation site was generated in exon 10 with a C insertion at the coding nucleotide position 1642. In addition, a *Bam*HI site was introduced at the coding nucleotides 1668–1673 without changing the amino acid sequence of the PV mutant. The neomycin resistance gene (*NeoR*), flanked by two *LoxP* sequences, was placed 1 kb downstream of the polyA site. The thymidine kinase gene (*TK*) was placed at the 3′ terminus of the targeting vector. The lengths of the 5′ and 3′ arms were 5.4 kb and 5.6 kb, respectively.

The targeting vector was linearized by *Xba*I digestion and transfected (25 $\mu$g) into the TC-1 embryonic stem cells (17). Recombinant clones were treated with 400 $\mu$g/ml G418 for positive selection and 2 $\mu$M gancyclovir for negative selection. Seven recombinant clones were identified by Southern blotting analysis. The clones were microinjected into C57BL/6J blastocysts to produce chimeras, which were crossed with NIH Black Swiss mice to establish germ-line transmission (18). Mice harboring the targeted *PV* mutation and the *NeoR* gene are designated as *TR$\beta$PVNeoR* mice (Fig. 1*C*).

*TR$\beta$PVNeoR* mice were genotyped by Southern blotting analyses and/or PCR by using two sets of primers. For the identification of the wild-type allele, the sequence of the 5′-primer (W5) is: 5′-TCCCCAAGCCAGCATCCCGACC, and the 3′-primer (W3) is: 5′-CGGGCAAATCCTTACCTGG. For the identification of the mutant allele, the 5′-mutant primer (M5) is: 5′-TGCAGTGGCGATGGCATC, and the 3′-primer (M3) is: 5′-CTGACCGCTTCCTCGTGCTTTACG. PCR reactions were carried out for 35 cycles (94°C, 30 sec; 59°C, 30 sec; 74°C; 30 sec for the determination of the wild-type allele) (94°C, 30 sec; 63°C, 30 sec; 74°C; 30 sec for the mutant allele) in a buffer containing $MgCl_2$ by using TaKaRa EX-*Taq* polymerase (Intergen, Purchase, NY).

To delete the *NeoR* gene from the targeted locus *in vivo*, *TR$\beta$PVNeoR* mice (Fig. 1*C*) were crossed with homozygous Ella-*Cre* transgenic mice (19). The resulting offspring were genotyped by Southern blot and PCR analyses by using primers W5 and W3. Mice harboring the targeted PV mutation, but without the *NeoR* gene, are designated as TR$\beta^{PV/PV}$ and TR$\beta^{PV/+}$ for the homozygous and heterozygous mutant mice, respectively.

**Determination of the Expression of PV Mutant RNA in Tissues by Reverse Transcription–PCR (RT-PCR).** Total RNA was prepared by using Trizol Reagent (Life Technologies, Rockville, MD). RT-PCR was carried out by using poly(dT) as a primer for cDNA synthesis by using SuperScript II reverse transcriptase (Life Technologies). Fragments (688 bp) from the wild-type *TR* or (689 bp) from the mutant *PV* were amplified in the presence of 5′-primer (primer N): 5′ ATGGGGAAATGGCAGTGACACGAG and 3′-primer (primer C): 5′-TGGGAGCTGGTGATGACTTCGTGC by using *Taq* DNA polymerase (Perkin–Elmer). The mutant *PV* sequence contained a *Bam*HI site that was not present in the mouse endogenous *TR$\beta$* gene. PCR products were digested with *Bam*HI to yield two 380- and 309-bp fragments for mutant *PV*, as analyzed by gel electrophoresis.

**Northern Blot Analyses.** Total RNA (5–10 $\mu$g) was used for Northern blot analysis. After electrophoresis, RNA was transferred onto membranes (Hybond-N+, Amersham Pharmacia), which were hybridized with appropriate probes. cDNA clones for TSH$\alpha$, TSH$\beta$, growth hormone (GH), malic enzyme (ME), spot 14, and 5′-deiodinase I (5′-DI-I) were labeled with [$\alpha$-$^{32}$P]dCTP by using a random primer hexamer protocol. For quantification, the intensities of the mRNA bands were normalized against the intensities of GAPDH mRNA ($n$ = 3). The blots were stripped and rehybridized with a $^{32}$P-labeled GAPDH cDNA. Quantifi-

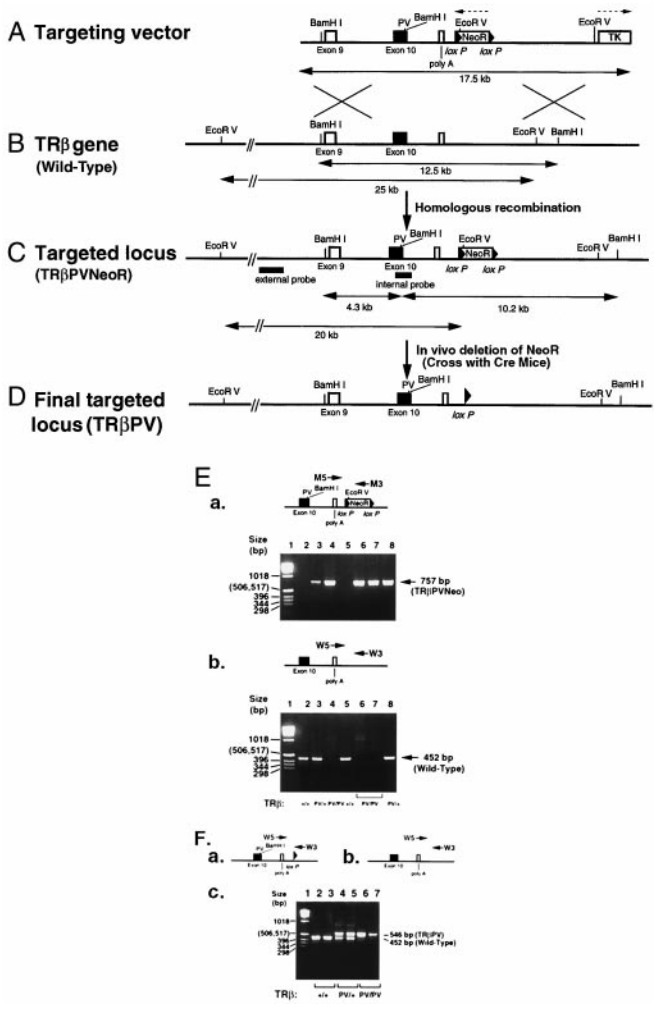


**Fig. 1.** Targeting of the *PV* mutation onto the *TR$\beta$* gene locus by homologous recombination. (*A*) Schematic representation of the *PV* targeting vector. The 17.5-kb targeting vector contains the *PV* mutation in exon 10. The locations of the *NeoR* (flanked by two LoxP sequences) and the *HSV-TK* genes are as indicated. The directions of transcription of *NeoR* and *HSV-TK* are indicated by dotted arrows. (*B*) Restriction map of the wild-type *TR$\beta$* gene locus. The expected size of the fragments digested by *Bam*HI and *Eco*R V, which were detected by internal and external probes (*C*), respectively, are indicated. (*C*) Targeting the *PV* mutation into the *TR$\beta$* gene locus via homologous recombination (*TR$\beta$PVNeoR*). The expected sizes of the fragments of the targeted locus digested by *Bam*HI and *Eco*RV, which were detected by the internal and external probes, are indicated. (*D*) The final targeted locus (*TR$\beta$PV*). The *NeoR* gene was deleted *in vivo* by crossing the *TR$\beta^{PV/PV}$NeoR* mice with *Ella-Cre* mice (19). (*E*) Genotyping of *TR$\beta$PVNeoR* mice. (*a*) Diagram: Primers used in the PCR analysis of *TR$\beta$PVNeoR* mice. Panel: PCR analysis of *TR$\beta$PVNeoR* mice. The 757-bp fragment from the *TR$\beta$PVNeoR* mice was detected when the pair of primers M5 and M3 was used in PCR. (*b*) In a separate PCR by using the genomic DNA from the same mice, the wild-type mice yielded a 452-bp fragment (panel) when the pair of primers W5 and W3 was used (diagram). From the two separate runs of PCR, the genotypes of *TR$\beta$PVNeoR* mice were determined. Lanes 2 and 5: wild-type mice; lanes 3 and 8: *TR$\beta^{PV/+}$NeoR* mice; lanes 4, 6 and 7: *TR$\beta^{PV/PV}$NeoR* mice. (*F*) Genotype analysis of *TR$\beta$PV* mice. Fragments (452 and 546 bp) obtained by PCR from (*a*) *TR$\beta$PV* and (*b*) wild-type mice. (*c*) The actual genotype analysis.

cation was performed by using the Molecular Dynamics Phosphor-Imager (Molecular Dynamics).

**Hormone Assays and Determination of Serum Cholesterol.** Serum levels [total L-thyroxine (T4) and T3] were determined by using Gamma Coat T4 or T3 assay RIA kit (DiaSolin, Stillwater, MN) according to the manufacturer's instructions. TSH levels in serum were measured as described (20).

**Histology and Immunohistochemistry.** Thyroid glands were fixed in 10% neutral buffered formalin and subsequently embedded in paraffin. Five-micrometer-thick sections were prepared and stained with hematoxylin and eosin for microscopic examination.

Pituitaries from $TR\beta^{PV/PV}$ mice and wild-type littermates were fixed in 10% formalin in PBS for 2 h at 23°C, dehydrated, and embedded in paraffin. Five-micrometer-thick sections were deparaffinized in xylene, washed in ethanol, then treated with antigen unmasking solution (Vector Laboratories) and heated in a microwave oven for 5 min. The sections were then blocked in 1% BSA in PBS for 30 min at 23°C, followed by sequential incubations in rabbit anti-mouse TSH antiserum [1:1,000 dilution in BSA–PBS; Biogenesis (Bournemouth, U.K., catalogue no. 8922-6009)] for 30 min at 23°C, washed with PBS, then incubated with affinity-purified goat anti-rabbit IgG conjugated to horseradish peroxidase (Jackson ImmunoResearch). After washing in PBS, the sections were incubated in diaminobenzidine substrate solution (10 min, 23°C) followed by dehydration and mounting under cover slips without counterstains. Unstained sections were then examined by using bright-field as well as phase-contrast microscopy, and digital images were captured from these sections by using a ×20 objective and a Dage 300 CCD camera with a Zeiss Axioplan 2 microscope. These images were then printed, and nuclei of all cells in the field were counted by using the phase contrast image. The cells showing TSH labeling were then counted in the parallel bright-field image of the same field. The total numbers of cells counted for the pituitaries from the $TR\beta^{PV/PV}$ and wild-type mice were 866 and 655, respectively.

**Data Analysis.** All data are expressed as mean ± SE. Statistical analyses used the student's $t$ test, and $P < 0.05$ was considered significant.

## Results

**Generation of Mice with Targeted *TRβ* Mutant PV.** The targeting vector is shown in Fig. 1*A*. Positive embryonic stem (ES) clones were identified by using both internal and external probes (Fig. 1 *B* and *C*). *Bam*HI digests of the genomic DNA from two positive clones revealed 12.5-, 10.2-, and 4.3-kb fragments when hybridized with the internal probe encompassing the PV mutation site in exon 10 (data not shown), whereas the control showed the expected 12.5-kb band (data not shown). When the *Eco*RV digests of the same positive ES clones were hybridized with the external probe, an additional 20-kb fragment was detected together with the 25-kb fragment derived from the wild-type allele (data not shown). These results indicate that the *PV* mutation was correctly targeted onto the *TRβ* gene locus.

Mice carrying the *TRβPVNeoR* gene (Fig. 1*C*) were identified by PCR by using DNA extracted from tails. By using primers for detection of mutant genes (M5 and M3; Fig. 1*E-a Upper*) or wild-type (W5 and W3; Fig. 1*E-b Upper*), typical results are shown in Fig. 1*E-a* and *b Lower*, respectively. The size of PCR products was 757 bp (lanes 3, 4, 6- 8 from different mice; Fig. 1*E-a Lower*) and 452 bp (lanes 2, 3, 5, and 8; Fig. 1*E-b Lower*) from the mutant and wild-type genes, respectively.

Northern blot analyses of *PV* gene expression in $TR\beta^{PV/+}NeoR$ heterozygous and $TR\beta^{PV/PV}NeoR$ homozygous mice (Fig. 1*C*) indicate that the expression of the *PV* mutant allele was repressed as compared with the wild-type *TRβ* allele (data not shown). Because the *NeoR* gene was flanked by two *loxP* sequences in the targeted locus (Fig. 1 *A* and *C*), it was possible to delete the *NeoR* gene *in vivo* by crossing the $TR\beta^{PV/PV}NeoR$ homozygous mice with an *Ella-Cre* mice (19). PCR analysis by using primers W5 and W3 (Fig. 1*F*) yielded a 546-bp fragment indicative of the removal of the *NeoR* gene (see Fig. 1 *B–D*). Mice with the final targeted locus [without *NeoR* gene (Fig. 1*D*)] were designated as $TR\beta^{PV/+}$ for the heterozygous mice and $TR\beta^{PV/PV}$ for the homozygous PV mutant mice.

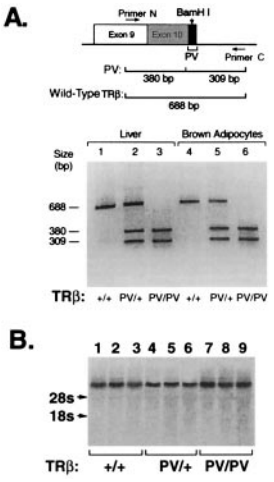


**Fig. 2.** Expression of PV mRNA in the liver and brown adipocytes. RT-PCR: Total RNA was isolated from liver (lanes 1–3) and brown adipocytes (lanes 4–6). RT-PCR was carried out by using the primers N and C as described in *Materials and Methods*. (*A*) Diagram: A 689- or 688-bp cDNA fragment was obtained from the mutant RNA and wild-type RNA, respectively. However, only the cDNA from the mutant RNA could be restricted with *Bam*HI to yield two 380- and 309-bp fragments. (*B*) Northern blot analysis. The probe was the mouse TRβ1 cDNA. Results were from three mice of each genotype, as marked.

**The *PV* Gene Is Expressed in All Expected Target Tissues Examined.** RT-PCR was used to assess the expression of the *PV* mutant allele at the RNA level. Primers flanking the mutated exon 10 were used, and the resultant cDNA was digested with *Bam*HI (Fig. 2*A Upper*). The cDNA derived from the mutant allele yielded two fragments with sizes 380 and 309 bp, whereas a 688-bp fragment was obtained from the wild-type mRNA. Fig. 2*A Lower* shows the representative mRNA expression patterns in the liver and brown adipocytes of $TR\beta^{PV/+}$ mice (lanes 2 and 5) and $TR\beta^{PV/PV}$ mice (lanes 3 and 6), respectively. This analysis shows that *PV* allele was expressed in the cerebrum, cerebellum, pituitary, heart, muscle, white adipocytes, lung, spleen, and kidney (data not shown), indicating that the *PV* mutant allele was detected in expected T3 target tissues.

The expression of the *PV* allele in the liver was further confirmed by Northern blot analysis by using a cDNA probe specific to the *TRβ* gene (Fig. 2*B*). Lanes 7–9 (from three mice) indicate that the level of the transcription of *TRβPV* gene in the $TR\beta^{PV/PV}$ mice was not significantly different from those in the $TR\beta^{PV/+}$ (lanes 4–6 for three mice) and in the wild-type $TR\beta^{+/+}$ littermates (lanes 1–3 for three mice). Similarly, expression of the *PV* and wild-type *TRβ* allele were similar in the heart and brain (data not shown). These findings indicate that the expression of the *TRβPV* gene was not affected by the presence of the *PV* mutation.

**Resistance to Thyroid Hormone Action on the Pituitary–Thyroid Axis.** Consistent with findings in heterozygous patients with the common form of RTH, the mean total T4 (TT4) concentration in $TR\beta^{PV/+}$ mice was 8.6 ± 0.4 μg/dl ($n = 9$), which is 2.5-fold higher than that

GENETICS

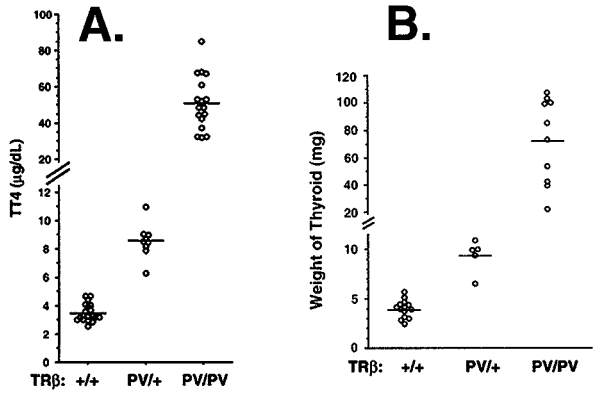


**Fig. 3.** Elevated levels of total T4 and enlarged thyroid glands in *TRβPV* mice. (*A*) Serum levels of total T4 in adult mice. (*B*) The corresponding sizes of thyroid glands. Each point represents a value for a single mouse and horizontal bars represent the mean values.

in the wild-type mice (3.5 ± 0.1 μg/dl; $n = 22$) (Fig. 3*A*). The 15-fold increase in the circulating TT4 (51 ± 3.6 μg/dl; $n = 17$) observed in the $TR\beta^{PV/PV}$ mice was similar to that observed in the single patient homozygous for a mutant *TRβ* gene (5).

The serum total T3 (TT3) concentration was also increased in *TRβPV* mice. The mean TT3 values for $TR\beta^{PV/+}$ and $TR\beta^{PV/PV}$ mice were 2.8 ± 0.17 ng/ml ($n = 23$) and 12.6 ± 1.3 ng/ml ($n = 16$), respectively. Compared with the TT3 of the wild-type mice (1.5 ± 0.1 ng/ml; $n = 18$), these T3 concentrations represent a 2- and 9-fold increase for the $TR\beta^{PV/+}$ and $TR\beta^{PV/PV}$, respectively.

The degree of thyroid gland enlargement was proportional to the magnitude of thyroid hormone elevation in serum of $TR\beta^{PV/+}$ and $TR\beta^{PV/PV}$ mice. As shown in Fig. 3*B*, the mean size of the thyroid gland (73 ± 9.8 mg; $n = 10$) from $TR\beta^{PV/PV}$ mice was ≈18-fold larger than that of the wild-type mice (4 ± 0.2 mg; $n = 14$). The mean size of the thyroid gland in $TR\beta^{PV/+}$ (9.4 ± 0.8 mg; $n = 5$) was 2.4-fold larger than that in the wild-type mice. Histological evaluation indicates a dramatic increase in the size of individual follicles in $TR\beta^{PV/+}$ (Fig. 4*B*) vs. wild-type mice (Fig. 4*A*) and extensive hyperplasia of the epithelium in $TR\beta^{PV/PV}$ mice (Fig. 4*C*).

Stimulation of TSH secretion also reflected the severity of RTH (Fig. 5*A*). In $TR\beta^{PV/+}$ mice, TSH was 2.1-fold higher (121.9 ± 24.8

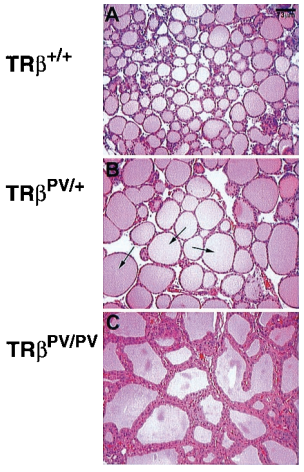


**Fig. 4.** Histology of thyroid glands of *TRβPV* mice. Extensive hyperplasia of the thyroid gland dissected from an 11-week-old female $TR\beta^{PV/PV}$ mouse (*C*) and a significant increase in follicle size in a $TR\beta^{PV/+}$ mouse (arrows, *B*), as compared with the histology of $TR\beta^{+/+}$ seen in *A* (×137).

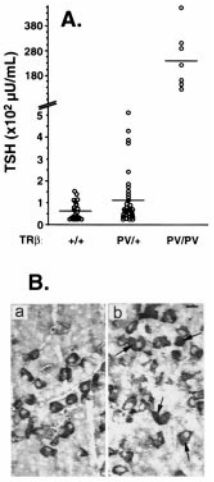


**Fig. 5.** Elevated serum TSH levels in *TRβPV* mice (*A*) and increases in the number of thyrotrophs (*B*). (*A*) Mean TSH levels in $TR\beta^{PV/+}$ and $TR\beta^{PV/PV}$ mice were 2.1- and 411-fold elevated in 3- to 4-month-old mice, respectively. The horizontal bars represent mean values. (*B*) TSH-secreting cells were increased in the pituitary of $TR\beta^{PV/PV}$ mice. TSH-positive cells, indicated by arrows, were counted. The number of cells counted in the pituitary of the wild-type $TR\beta^{+/+}$ (*a*) and $TR\beta^{PV/PV}$ mice (*b*) were 866 and 655, respectively.

microunits/ml; $n = 29$) as compared with the wild-type mice (58 ± 8.9 microunits/ml; $n = 21$). These results indicate that the pituitary is resistant to the action of thyroid hormone because $TR\beta^{PV/+}$ mice had 2.5-fold higher TT4 and 2-fold elevated TT3. A remarkable resistance was observed in the $TR\beta^{PV/PV}$ mice, showing a 412-fold higher serum TSH level (23,887 ± 4,408 microunits/ml; $n = 7$) in the presence of 15- and 9-fold increase in serum TT4 and TT3 levels, respectively. Again, similarly extraordinary increase (≈400-fold the normal) in the level of serum TSH was noted in the patient homozygous for a mutated *TRβ* gene (5).

We also examined whether the distribution of TSH secreting cells in the pituitary was affected by the expression of the *PV* mutant (Fig. 5*B*). By using an anti-TSH antibody, we found that the percentages of positively staining cells were 11.29 ± 0.76 ($n = 866$), 10.7 ± 2.0 ($n = 751$), and 19.31 ± 3.63 ($n = 655$) for the wild-type, $TR\beta^{PV/+}$, and $TR\beta^{PV/PV}$ mice, respectively. Even though the percentage of TSH positive cells was higher in the $TR\beta^{PV/PV}$ mice, the histologic pattern of distribution of thyrotrophs was not significantly different from normal with no localized foci of selective hyperplasia. The similar percentage of thyrotrophs in the pituitaries of $TR\beta^{PV/+}$ and $TR\beta^{+/+}$ mice indicates resistant response to the elevated of thyroid hormones in $TR\beta^{PV/+}$ mice. The ≈2-fold increase in the number of thyrotrophs likely accounts for up-regulation in the synthesis of TSH because of the action of mutant PV in the pituitary. Taken together, it is clear that the PV mutant interfered with the normal regulatory functions of wild-type TR in the pituitary.

**Retarded Growth in *TRβPV* Mice.** Growth retardation in *TRβPV* mice was manifested as delayed bone development and impaired weight gain. As shown in Fig. 6*A*, the mean lengths of tibias were 18.4 ± 0.2 mm ($n = 10$), 17.6 ± 0.1 mm ($n = 8$), and 16.6 ± 0.2 mm ($n = 6$) for $TR\beta^{+/+}$, $TR\beta^{PV/+}$, and $TR\beta^{PV/PV}$ mice, respectively. Compared with the wild-type mice, these were significant reductions of 10% and 5% in the lengths of tibias of $TR\beta^{PV/PV}$ and $TR\beta^{PV/+}$ mice, respectively. Similarly, the mean lengths of femurs were 15.6 ± 0.1 mm ($n = 10$), 15.1 ± 0.1 mm ($n = 8$), and 13.8 ± 0.2 mm ($n = 6$) for $TR\beta^{+/+}$, $TR\beta^{PV/+}$, and $TR\beta^{PV/PV}$ mice, respectively (Fig. 6*B*). These values represent significant reductions of 12% and 4% in the lengths of femurs for $TR\beta^{PV/PV}$ and $TR\beta^{PV/+}$ mice, respectively. The

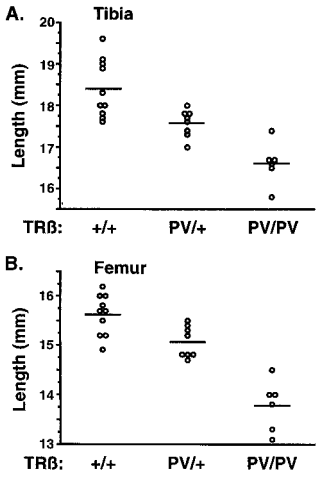


**Fig. 6.** Delayed bone development in *TRβPV* mice. (*A*) Lengths of tibias and (*B*) femurs show significant delayed bone development in $TR\beta^{PV/+}$ and $TR\beta^{PV/PV}$ mice.

abnormalities in bone development seen in *TRβPV* mice were not detected in $TR\beta^{-/-}$ mice (21).

Impaired weight gain was detected in both male and female $TR\beta^{PV/PV}$ mice. $TR\beta^{PV/PV}$ mice were smaller (17–23%) than wild-type $TR\beta^{+/+}$ littermates at all ages examined. $TR\beta^{PV/PV}$ mice also exhibited a reduced growth spurt by 25–40% during the age 3–7 weeks (data not shown). However, no significant differences in pup weights and growth rates were detected between $TR\beta^{PV/+}$ and $TR\beta^{+/+}$ mice (data not shown).

**Alteration in the Expression Patterns of T3-Target Genes in Tissues of *TRβPV* Mice.** As a first step to understand the molecular action of PV *in vivo*, we evaluated the expression of T3 target genes in the tissues of *TRβPV* mice. Fig. 7*A* shows the expression of TSH and GH mRNA in the pituitary gland. TSH consists of two polypeptides, the TSH-specific $\beta$ subunit and the common $\alpha$-glycoprotein subunit ($\alpha$-SU; also a subunit for gonadotropins), whose expression is suppressed by T3. However, despite the high circulating thyroid hormone levels, Northern blot analysis indicates that $\alpha$-SU mRNA levels in the pituitaries of $TR\beta^{PV/PV}$ and $TR\beta^{PV/+}$ mice were 60- and 1.7-fold higher than that of the wild-type mice (Fig. 7*A*). A lesser but significant effect of the *PV* mutant on the expression of the *TSHβ* gene was also observed (Fig. 7*A*). The TSH$\beta$ mRNA level in the pituitaries of $TR\beta^{PV/PV}$ mice was 2.7-fold higher than that in the wild-type mice. The TSH$\beta$ mRNA level in the $TR\beta^{PV/+}$ mice was not repressed as it should be by the elevated thyroid hormone levels, suggesting a reduced hormone-mediated repression of TSH$\beta$ mRNA in the presence of PV. The latter results clearly indicate the interference of PV mutant with the gene regulatory function of the wild-type receptors on the expression of these *α-SU* and *TSHβ* genes, albeit more pronounced for *α-SU* gene.

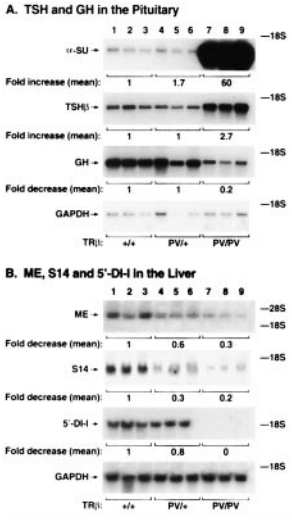


**Fig. 7.** The expression of T3-target genes in *TRβPV* mice was altered. Total RNA was isolated from the pituitaries and liver of mice (three for each group of 8-week-old male mice). The intensities of the bands were quantified by using a Molecular Dynamics PhosphorImager. The levels of expression of both genes were normalized by using GAPDH mRNA. The mean values of three experiments are shown and expressed as the fraction (fold) change from the value in the $TR\beta^{+/+}$ mice.

We further carried out Northern blot analyses of the positively T3-regulated genes in the pituitary. As shown in Fig. 7*A*, instead of being activated by the presence of the high circulating thyroid hormone levels, the expression of GH in the pituitaries of $TR\beta^{PV/PV}$ mice was repressed to 20% of that seen in the wild-type mice. The GH mRNA level in the $TR\beta^{PV/+}$ mice was not increased compared with the wild-type mice, showing a reduced GH mRNA response to the elevated thyroid hormone levels resultant from the presence of one single *PV* allele. Taken together, these results indicate that the response to thyroid hormone of both positively and negatively T3-regulated genes is attenuated in the pituitary of *TRβPV* mice.

The positively T3-regulated genes in the liver of *TRβPV* mice also show reduced expression. As shown in Fig. 7*B*, the expression of *ME, S14*, and *5′-DI-I* genes was reduced to 0.2, 0.3, and 0.8 in $TR\beta^{PV/+}$ mice, respectively, compared with wild-type mice. The expression of ME and S14 mRNA was further reduced in the $TR\beta^{PV/PV}$ mice (decreased to 0.3 and 0.2, respectively). No 5′-DI-I mRNA was detected in $TR\beta^{PV/PV}$ mice (Fig. 7*B*). These results indicate that the expression of *PV* gene dampened the magnitude of the T3-mediated responses of target genes in different tissues. These findings are in contrast to that found in mice lacking *TRβ* ($TR\beta^{-/-}$), in which no changes in the expression of ME genes were detected (22).

## Discussion

Consistent with the findings in heterozygous patients with RTH, $TR\beta^{PV/+}$ mice exhibited mild impairment in the pituitary–thyroid axis. $TR\beta^{PV/+}$ mice had a 2.1-fold elevated TSH despite 2- to 3-fold higher thyroid hormone levels as compared with $TR\beta^{+/+}$ mice. Corresponding increases in serum TSH, T4 and T3 in humans with RTH are on the average of 1.7-, 2.3-, and 2.5-fold, respectively (4). The thyroid glands showed enlarged follicles, and the development of bones was delayed. In $TR\beta^{PV/PV}$ mice, more extensive and pronounced abnormalities were observed. A severe resistance to the action of thyroid hormone in the pituitary was revealed by an extraordinarily high TSH level (412-fold increase) despite 9- to 15-fold increases in circulating T3 and T4 concentrations, respectively. The increases are also compatible with those reported in the single patient homozygous for a mutant *TRβ* (5). The thyroid gland exhibited extensive hyperplasia and an 18-fold increase in size. The growth in $TR\beta^{PV/PV}$ mice was severely impaired, with a ≈17–23% reduction in weight gain and a ≈10% decrease in the lengths of long bones. These abnormalities are reminiscent of the findings in the patient with homozygous mutated *TRβ* alleles (5). These results indicate that the mouse with a targeted *PV* mutation described in the present study is an accurate model for the study of RTH. In contrast to the previously reported transgenic mice (10–14), the present mouse model provides an opportunity for future in-depth analysis of the molecular basis of RTH, which has not been possible in humans.

Although the mild impairment in the thyroid–pituitary axis of $TR\beta^{PV/+}$ mice is similar to that exhibited by the mice lacking $TR\beta$, there are clear differences in the phenotypes between $TR\beta^{PV/PV}$ and $TR\beta^{-/-}$ mice (21). The latter have neither severe dysfunction of the pituitary–thyroid axis nor impairment in weight gain and bone development. This study demonstrates that in mouse as in human, the effects of absence of $TR\beta$ are distinct from those of the presence of a mutant $TR\beta$. The present study shows that PV interferes with gene regulatory functions of the wild-type receptors *in vivo* (Fig. 7 *A* and *B*). Despite higher levels of thyroid hormone in $TR\beta^{PV/PV}$ mice, the responses of T3-regulated genes are attenuated. Thus, PV attenuated the expression of genes positively regulated by thyroid hormone including the *GH* gene in the pituitary and the *ME, S14,* and *5′-DI-I* in the liver. The expression of TSH mRNAs was activated, instead of being repressed by high T3 and T4, as demonstrated in hypothyroid mice treated with thyroid hormones (23). However, in contrast to that observed in hypothyroid mice (23, 24), the up-regulation of *α-SU* mRNA was more pronounced than TSH$\beta$ mRNA in *TRβPV* mice. At present, it is not clear whether this was because of T3-independent functions and/or the gene-specific actions of PV.

Several mechanisms, however, have been proposed to explain the interference of the mutant TR$\beta$ with the gene regulatory functions of the wild-type receptors: (*i*) competition for binding to TRE; (*ii*) exhaustion of limited transcription factors; or (*iii*) formation of inactive wild-type/mutant heterodimers on TRE. On the basis of the available *in vitro* biochemical evidence, the mechanism of competition of the wild-type TRs with mutants for binding to TRE is currently favored (mechanism *i*) (7, 25). However, the present *in vivo* data suggest that the possibility of formation of inactive wild-type/mutant heterodimers on TRE is also a viable mechanism (mechanism *iii*). In $TR\beta^{PV/+}$ mice, with the presence of one copy of TR$\beta$ (from the remaining one wild-type allele) and TR$\alpha$1 (from two $TR\alpha$ alleles), the expressed PV receptor probably preferentially forms inactive TR$\beta$/PV heterodimers on the TREs of T3 target genes. Detailed biochemical analyses have shown that mutant PV forms inactive heterodimers with wild-type TR$\beta$ or TR$\alpha$1 and that the former is preferred because of a higher affinity in the dimer formation (26). The mild phenotype exhibited in the pituitary–thyroid axis of the $TR\beta^{PV/+}$ mice as a result of the antagonism of the TR$\beta$-mediated functions by the preferential formation of inactive TR$\beta$/PV heterodimers is reminiscent of the phenotype seen in the mice lacking $TR\beta$ (21). The severe phenotype observed for the $TR\beta^{PV/PV}$ mice most likely represents a combination of the loss of both TR$\beta$- and TR$\alpha$1-mediated functions. The former is because of the loss of the two wild-type $TR\beta$ alleles, and the latter is because of the interference of PV mutant on the functions of TR$\alpha$1, presumably via the formation of inactive TR$\alpha$1/mutant heterodimers in the absence of TR$\beta$1 proteins. This hypothesis is supported by a similar degree of severe impairment in the pituitary–thyroid axis seen in mice deficient in both $TR\alpha$ and $\beta$ ($TR\alpha^{-/-}TR\beta^{-/-}$; refs. 27, 28).

It is important, however, to point out that the mechanisms underscoring the similar hyperactivity of the pituitary–thyroid axis and growth impairment seen in the $TR\alpha^{-/-}TR\beta^{-/-}$ mice (27, 28) and $TR\beta^{PV/PV}$ mice are totally different. The former is because of the lack of receptor alleles (27, 28), and the latter is because of the interference of the mutant receptor with the functions of wild-type receptors. Before all of the affected thyroid hormone target organs are evaluated and compared, it is premature to conclude that all other phenotypes exhibited by these two mouse models will be similar. It is entirely possible that the effects of mutant receptor *in vivo* could also manifest as "gain of function," which could contribute to the phenotype seen in the *TRβPV* mice. Therefore, future analyses and comparison of the phenotypes of these two mouse models should shed light on the mechanisms of actions of the wild-type and mutant receptors.

We are grateful for the expert technical assistance provided by W. Vieira. We thank D. Gong for assistance in obtaining the mouse genomic P1 clone of the *TRβ* gene from Genome Systems, D. Forrest for providing the unpublished partial genomic restriction maps 12 kb down-stream of exon 10 of the *TRβ* gene, and E. Chester Ridgway and W. Wood for the mouse TR genomic plasmids (pWD5 and pWD67) and the expression plasmids of mouse TR$\alpha$1 and TR$\beta$1. We thank H. Westphal for providing the *Ella-Cre* mice (Laboratory of Mammalian Genes and Development, National Institute of Child Health and Human Development, National Institutes of Health), P. McPhie for the analysis of growth rate of TR$\beta$PV mice, and J. Robbins for critical reading of the manuscript. M.K. is supported in part by the Japan Society for the Promotion of Science Research Fellowship for Japanese Biomedical and Behavioral Researchers at the National Institutes of Health. S.R. is supported in part by grant DK15070 from the National Institutes of Health.

1. Oppenheimer, J. H., Schwartz, H. L. & Strait, K. A. (1994) *Eur. J. Endocrinol.* **130,** 15–24.
2. Cheng, S. Y. (1995) *J. Biomed. Sci.* **2,** 77–89.
3. Shibata, H., Spencer, T. E., Onate, S. A., Jenster, G., Tsai, S. Y., Tsai, M. J. & O'Malley, B. W. (1997) *Recent Prog. Horm. Res.* **52,** 141–164.
4. Refetoff, S., Weiss, R. E. & Usala, S. J. (1993) *Endocr. Rev.* **14,** 348–399.
5. Ono, S., Schwartz, I. D., Mueller, O. T., Root, A. W., Usala, S. J. & Bercu, B. B. (1991) *Clin. Endocrinol. Metab.* **73,** 990–994.
6. Sakura A., Miyamoto T., Refetoff S. & DeGroot, L. J. (1990) *Mol. Endocrinol.* **4,** 1988–1994.
7. Yen, P. M. & Chin, W. W. (1994) *Mol. Endocrinol.* **8,** 1450–1454.
8. Tagami T., Gu W. X., Peairs P. T., West B. L., Jameson, J. L. (1998) *Mol. Endocrinol.* **12,** 1888–1902.
9. Collingwood, T. N., Wagner, R., Matthews, C. H., Clifton-Bligh, R. J., Gurnell, M., Rajanayagam, O., Agostini, M., Fletterick, R. J., Beck-Peccoz, P., Reinhardt, W., *et al.* (1998) *EMBO J.* **17,** 4760–4770.
10. Wong, R., Vasilyev, V. V., Ting, Y. T., Kutler, D. I., Willingham, M. C., Weintraub, B. D. & Cheng, S. (1997) *Mol. Med.* **3,** 303–314.
11. Hayashi, Y., Xie, J., Weiss, R. E., Pohlenz, J. & Refetoff, S. (1998) *Biochem. Biophys. Res. Commun.* **245,** 204–210.
12. Abel, E. D., Kaulbach, H. C., Campos-Barros, A., Ahima, R. S., Boers, M. E., Hashimoto, K., Forrest, D. & Wondisford, F. E. (1999) *J. Clin. Invest.* **103,** 271–279.
13. Gloss, B., Sayen, M. R., Trost, S. U., Bluhm, W. F., Meyer, M., Swanson, E. A., Usala, S. J. & Dillmann, W. H. (1999) *Endocrinology* **140,** 897–902.
14. Zhu, X. G., Kaneshige, M., Parlow, A. F., Chen, E., Hunziker, R. D., McDonald, M. P. & Cheng, S. Y. (1999) *Thyroid* **9,** 1137–1145.
15. Parrilla, R. A., Mixson, A. J., McPherson, J. A., McClaskey, J. H. & Weintraub, B. D. (1991) *J. Clin. Invest.* **88,** 2123–2130.
16. Bhat, M. K., McPhie, P., Ting, Y. T., Zhu, X.-G. & Cheng, S.-y. (1995) *Biochemistry* **34,** 10591–10599.
17. Barlow, C., Hirotsune, S., Paylor, R., Liyanage, M. Eckhaus, M., Collins, F., Shiloh, Y., Crawley, J. N., Ried, T., Tagle, D. & Wynshaw-Boris, A. (1996) *Cell* **86,** 159–171.
18. Deng, C. X., Wynshaw-Boris, A., Shen, M. M., Daugherty, C., Ornitz, D. M. & Leder, P. (1994) *Genes Dev.* **8,** 3045–3057.
19. Lakso, M., Pichel, J. G., Gorman, J. R., Sauer, B., Okamoto, Y., Lee, E., Alt, F. W. & Westphal, H. (1996) *Proc. Natl. Acad. Sci. USA* **93,** 5860–5865.
20. Pohlenz J., Weiss R. E., Cua K., Van Sande J. & Refetoff, S. (1999) *Thyroid* **9,** 1265–1271.
21. Forrest, D., Hanebuth, E., Smeyne, R. J., Everds, N., Stewart, C. L., Wehner, J. M. & Curran, T. (1996) *EMBO J.* **15,** 3006–3015.
22. Weiss, R. E., Murata, Y., Cua, K., Hayashi, Y., Seo, H. & Refetoff, S. (1998) *Endocrinology* **139,** 4945–4952.
23. Chin, W. W., Shupnik M. A., Ross D. S., Habener, J. F. & Ridgway, E. C. (1985) *Endocrinology* **116,** 873–878.
24. Shibusawa, N., Yamada, M., Hirato, J., Monden, T., Satoh, T. & Mori, S. (2000) *Mol. Endocrinol.* **14,** 137–146.
25. Meier, C. A., Dickstein, B. M., Ashizawa, K., McClaskey, J. H., Muchmore, P., Ransom, S. C., Menke, J. B., Hao, E. H., Usala, S. J., Bercu, B. B., *et al.* (1992) *Mol. Endocrinol.* **6,** 248–258.
26. Zhu, X. G., McPhie, P. & Cheng, S. Y. (1997) *Endocrinology* **137,** 712–721.
27. Gothe, S., Wang, Z., Ng, L., Kindblom, J. M., Barros, A. C., Ohlsson, C., Vennstrom, B. & Forrest, D. (1999) *Genes Dev.* **13,** 1329–1341.
28. Gauthier, K., Chassande, O., Plateroti, M., Roux, J. P., Legrand, C., Pain, B. Rousset, B., Weiss, R., Trouillas, J. & Samarut, J. (1999) *EMBO J.* **18,** 623–631.